

## Article

# Scanning Electrochemical Microscopy-Somatic Cell Count as a Method for Diagnosis of Bovine Mastitis

Shigenobu Kasai <sup>1,\*</sup>, Ankush Prasad <sup>2,\*</sup> , Ryoma Kumagai <sup>1</sup> and Keita Takanohashi <sup>1</sup>

<sup>1</sup> Graduate Department of Electronics, Tohoku Institute of Technology, Sendai 982-8577, Japan; m181803@st.tohtech.ac.jp (R.K.); s1811242@st.tohtech.ac.jp (K.T.)

<sup>2</sup> Department of Biophysics, Faculty of Science, Palacký University, 783 71 Olomouc, Czech Republic

\* Correspondence: kasai@tohtech.ac.jp (S.K.); ankush.prasad@upol.cz (A.P.)

**Simple Summary:** Mastitis is inflammation/swelling in the breast, which is generally caused by an infection. In this study, we present scanning electrochemical microscopy-somatic cell count (SECM-SCC) as a novel method for diagnosis of mastitis in bovines. We developed a biosensor in this study that can serve as a highly promising portable electrochemical device for mastitis diagnosis in bovines.

**Abstract:** The method to diagnose mastitis is generally the somatic cell count (SCC) by flow cytometry measurement. When the number of somatic cells in raw milk is  $2.0 \times 10^5$  cells/mL or more, the condition is referred to as mastitis. In the current study, we created a milk cell chip that serves as an electrochemical method that can be easily produced and used utilizing scanning electrochemical microscopy (SECM). The microelectrode present in the cell chip scans, and the difference between the oxygen concentration near the milk cell chip and in bulk is measured as the oxygen (O<sub>2</sub>) reduction current. We estimated the relationship between respiratory activity and the number of somatic cells in raw milk as a calibration curve, using scanning electrochemical microscopy-somatic cell count (SECM-SCC). As a result, a clear correlation was shown in the range of  $10^4$  cells/mL to  $10^6$  cells/mL. The respiration rate (F) was estimated to be about 10–16 mol/s per somatic cell. We also followed the increase in oxygen consumption during the respiratory burst using differentiation inducer phorbol 12-myristate 13-acetate (PMA) as an early stage of mastitis, accompanied with an increase in immune cells, which showed similar results. In addition, we were able to discriminate between cattle with mastitis and without mastitis.

**Keywords:** mastitis; bovines; cows; somatic cell count; respiratory activity



**Citation:** Kasai, S.; Prasad, A.; Kumagai, R.; Takanohashi, K. Scanning Electrochemical Microscopy-Somatic Cell Count as a Method for Diagnosis of Bovine Mastitis. *Biology* **2022**, *11*, 549. <https://doi.org/10.3390/biology11040549>

Academic Editor: José Luis Toca-Herrera

Received: 23 February 2022

Accepted: 31 March 2022

Published: 1 April 2022

**Publisher's Note:** MDPI stays neutral with regard to jurisdictional claims in published maps and institutional affiliations.



**Copyright:** © 2022 by the authors. Licensee MDPI, Basel, Switzerland. This article is an open access article distributed under the terms and conditions of the Creative Commons Attribution (CC BY) license (<https://creativecommons.org/licenses/by/4.0/>).

## 1. Introduction

Bovine mastitis leads to inflammation in the mammary glands [1–3]. It is caused by the invasion and proliferation of pathogenic microorganisms from the teat opening into the mammary gland [4]. Mastitis is said to be one of the largest problems in the dairy industry [3,5,6], and about 380,000 cases occur annually in Japan, accounting for about 30% of all dairy cow injuries. The detection and treatment of asymptomatic latent mastitis is crucial for reducing economic losses. It has been reported that the number of somatic cells in raw milk ranges somewhere between  $1.0$ – $2.5 \times 10^5$  cells/mL for categorizing or treating latent mastitis. Therefore, in this manuscript, the number of somatic cells in raw milk is taken as normal when it is less than  $1.0 \times 10^5$  cells/mL and subclinical/latent mastitis when it is in the range of  $1.0 \times 10^5$  cells/mL to  $2 \times 10^5$  cells/mL. The value  $2 \times 10^5$  cells/mL or more is treated as clinical mastitis. These limits are highly variable, depending on the geographical region. In most developed dairy industries, for instance, the European Union, directives have set a limit of 400,000 cells/mL for SCC in raw buffalo milk, while in United States, this limit is set to 750,000 cells/mL. Somatic cell count in cow milk >200,000 cells/mL indicates mastitis according to the directives of the International Dairy Federation [7,8].

It is also estimated to cause an annual economic loss of \$2 billion in the United States [9]. In the early stages of mastitis, the number of leukocytes in raw milk (further referred to as milk in the text) increases to combat the bacteria that have invaded the mammary gland, and the number of somatic cells in milk increases to about  $10^5$  cells/mL. As the condition progresses, cells on the surface of the mammary gland that have died due to inflammation are shed, and the number of somatic cells in milk increases to about  $10^6$  cells/mL. The number of somatic cells in milk is used as an index for mastitis detection, and many testing methods have been developed [10–15]. Three typical somatic cell count evaluation methods are widely known. The first method, the California mastitis test (CMT) [16], is a method of visually observing and discriminating a gelled sample by destroying the cell membrane of somatic cells in milk and reacting DNA with a chemical reagent. This method is simple and does not require a device or complicated operation and is used as a simple inspection method in farms; however, it is difficult to distinguish between healthy bovines and early mastitis bovines because it is judged by colour and shape, and thus early detection is difficult [17]. The second method is a test method that measures the electrical conductivity of milk [18,19]. This method is rather simple and is incorporated in milking machines and milk parlours; however, the value changes due to environmental fluctuations such as temperature rather than cells. It is difficult to measure accurately using this method. The third method is a somatic cell count (SCC) method [20] that uses flow cytometry, which during the past decade has been widely used as a mastitis test method to directly count individual cells [3]. It is quantitative, while CMT and electrical conductivity are qualitative methods. By this method, the cattle are determined to have mastitis when the number of somatic cells in milk is  $2.0 \times 10^5$  cells/mL or more, and caution is required when the number of cells in milk ranges between  $10^5$  cells/mL and  $10^6$  cells/mL [21,22]. Since this measuring device is large and expensive, it is difficult to install in each parlour. In Japan, it is typical to send raw milk to a testing facility to perform this test, and thus real-time testing is difficult on a daily basis, making early detection challenging. In recent years, as a method for monitoring the increase in leukocytes in the early stage of mastitis for earlier detection, inflammatory cytokine evaluation [23,24], measurement of hydrogen peroxide ( $H_2O_2$ ) using chemiluminescence method [25], etc., have been used. A method for evaluating superoxide anion radicals, which is one of the reactive oxygen species (ROS), was also developed [26]. However, these methods require expensive reagents such as antibodies and enzymes.

Aiming for the development of a bovine mastitis test method that can be easily tested by dairy farmers in real time, we decided to study an electrochemical method that can measure using a small amount of sample and inexpensive reagent. Scanning electrochemical microscopy (SECM) [27,28] using a microelectrode as a probe has been used for single-cell studies [29,30] and single-molecule level measurements in the past [31]. Since cells in body fluids and culture fluids consume oxygen during respiration, the dissolved oxygen concentration of the solution in the vicinity decreases, and a diffusion layer is formed due to the difference in concentration. The dissolved oxygen (DO) concentration in the solution can be measured as an oxygen reduction current by applying a voltage to the platinum microelectrode of the SECM probe. Using SECM, Shiku et al. scanned the microelectrode up and down in the Z-axis direction to evaluate the quality of fertilized bovine embryos by measuring respiratory activity [29]. Recently, Kaya et al. measured the correlation between the number of bacteria in collagen-embedded culture and respiration activity [32]. In addition, we also evaluated the respiration activity and respiratory bursts of human cells in our studies [33–35].

The current study examines whether it is possible to monitor the increase in leukocytes in early bovine mastitis through evaluation of respiratory activity. In addition, imaging the 3D distribution of respiration activity by SECM can be used as a simple test by a dairy farmer in real time. We first standardized the centrifugation conditions to avoid electrode adsorption by milk components, devised cell chipping and the hemispherical diffusion distribution by SECM, and examined whether there was a correlation between

respiratory activity taking into account cell count and the number of somatic cells in milk. Furthermore, we created a calibration curve for measuring the number of somatic cells by evaluating the respiration activity of  $10^4$  to  $10^6$  cells/mL, which is necessary for bovine mastitis testing. The calibration curve needs to be extended with more data points and to reach saturation. In addition, we also investigated whether SECM-SCC can detect increased oxygen consumption under induced respiratory bursts specifically caused by immune cells such as monocytes and neutrophils. As an output, the current work led to the development of a new simple test method for bovine mastitis.

## 2. Materials and Methods

### 2.1. SECM-SCC with Inverted Cone-Shaped Well

Figure 1 shows a conceptual diagram of the simple bovine mastitis test method performed in this study. Milk collected from bovines in Figure 1A contained fat (4%) and protein (3%) in addition to somatic cells. Centrifugation was required (as shown in the photograph of the centrifuge tube in (A) to remove these components (fat and proteins). An equal volume (5 mL each) of blood cell separation solution was mixed with milk and centrifuged at 1726 rpm for 30 min, and the supernatant containing fats and protein (~9 mL) was removed. Furthermore, a second centrifugation (1544 rpm, 10 min) was done by adding 3 mL of 11.4 mM glucose-containing phosphate buffer saline (PBS) to remove the blood cell separation solution. The precipitate suspended in a small volume of buffer (cell-aggregated milk somatic cells) was then used for measurement. We took 10  $\mu$ L of the sample on a hemocytometer and counted the number of cells. The samples were adjusted to  $6.00 \times 10^6$  cells/mL and  $6.00 \times 10^5$  cells/mL. The number of somatic cells in raw milk was measured using the hemocytometer to distinguish between the cells and fat globules. The photograph (Figure 1B, lower panel) shows a photomicrograph of milk before centrifugation, and the photograph on the right shows a photomicrograph of the cell suspension after centrifugation. Somatic cells with a diameter of about 10 to 20  $\mu$ m can be observed.

For measurements, 8  $\mu$ L of sample was taken in an inverted cone-shaped well (diameter ( $\phi$ ) 4 mm, depth 2 mm) and allowed to stand for 15 min. Following that, a platinum microelectrode ( $\phi$  20  $\mu$ m) was used as the working electrode; Ag/AgCl was used as the counter electrode and reference electrode. A total of 10 mL of 11.4 mM glucose-containing PBS was used as the measurement solution. As presented in Figure 1C, we measured the difference in oxygen reduction current between surface and bulk by sweeping back and forth vertically (referred to as z-scan) while applying a voltage to the microelectrode. We evaluated the respiratory activity of cells from the difference in current value by scanning electrochemical microscopy-somatic cell count (SECM-SCC). The platinum microelectrode was held 20  $\mu$ m above the cell suspension at an applied voltage of  $-0.5$  V vs. Ag/AgCl and scanned 1000  $\mu$ m in the Z direction while measuring the oxygen reduction current. The scan rate was kept at 10  $\mu$ m/s; the number of scans was 3 and the sampling time was 100 ms. The microelectrode reciprocated between a position (surface) about 20  $\mu$ m above the surface of the cone-shaped well and about 1020  $\mu$ m (bulk) at intervals of 200 s.

### 2.2. Evaluation of Electrodes over Time: Validating Stability Using Cyclic Voltammetry Measurements

Cyclic voltammetry (CV) was performed to evaluate the change in the value of current over time to investigate the cause of the difficulty in measuring respiration activity at the above-mentioned cell count of  $10^4$  cells/mL or less. The CV of the Pt microelectrode was measured using 4 mL of 4 mM potassium ferrocyanide solution as the measurement solution and Ag/AgCl as the counter electrode and reference electrode, respectively. We measured the oxygen reduction current at a sample-electrode distance of 20  $\mu$ m. The CV of the Pt microelectrode at 1, 3, 5, and 10 min after the start of measurement was compared with the CV of the Pt microelectrode before measurement. In addition, to observe the change in the current value, a cleaning pulse (Figure 1D) was applied to the electrode, and cyclic voltammetry was performed again (with 12 repetitions). Somatic cells that had been

centrifuged and removed from milk were mixed with collagen gel at a ratio of 1:9, and 8  $\mu\text{L}$  was poured in an inverted cone-shaped well. A Pt microelectrode ( $\phi$  20  $\mu\text{m}$ ) was used as the working electrode, Ag/AgCl was used as the counter electrode and reference electrode, and 10 mL of 11.4 mM glucose-containing PBS was used as the measurement solution. The sample-electrode distance was fixed at 20  $\mu\text{m}$ . In this state, the oxygen reduction current was measured for 10 min. Before and after this measurement, cyclic voltammetry of 0.0~0.7 V vs. Ag/AgCl at 20 mV/s was performed using 4 mM  $\text{K}_4\text{Fe}(\text{CN})_6$ -containing PBS to evaluate the effect of the collagen embedding treatment.

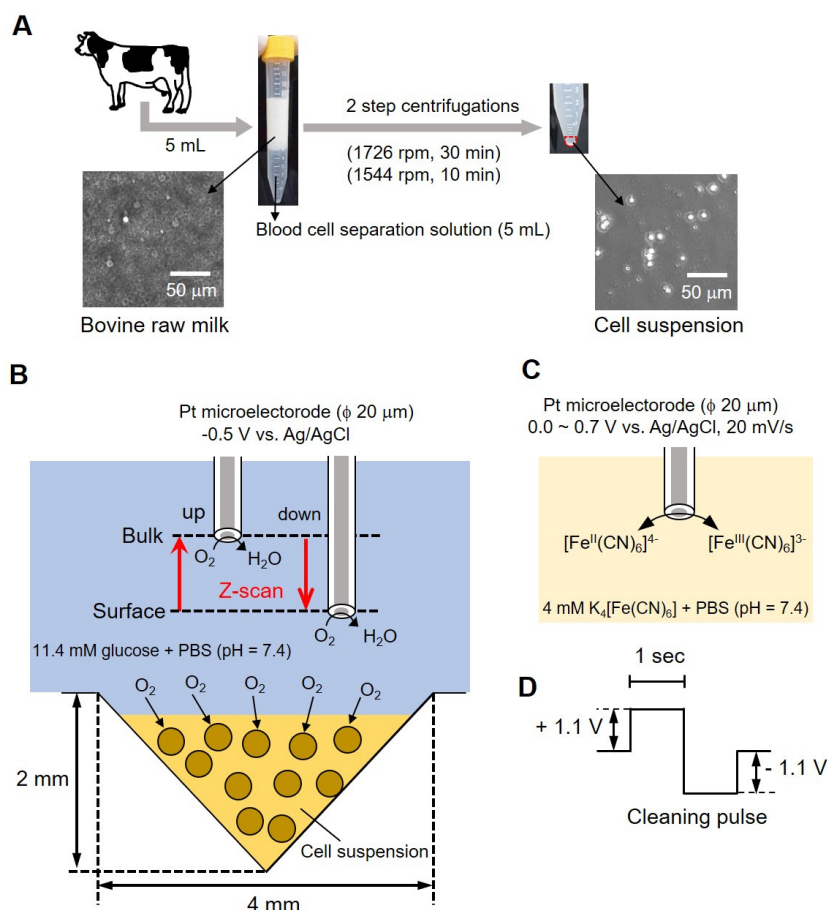


**Figure 1.** Conceptual diagram of bovine mastitis test methodology. Centrifugal method of the bovine milk (A); conceptual diagram of the evaluation of somatic cell respiration activity by measuring the oxygen reduction current value (B); reaction mechanism at the platinum electrode (C) and cleaning pulse (D).

### 2.3. Cell Biochip to Obtain the Sensitivity Required for SECM-SCC

A silicon substrate having an inverted pyramid-shaped fine groove was produced by anisotropic etching, which is a three-dimensional microfabrication technique. The lower surface ( $200 \times 200 \mu\text{m}$ ) of this well should be in  $\mu\text{m}$  size that can be easily measured by SECM, and this surface is used as the detection port. In addition, the upper surface ( $1550 \times 1550 \mu\text{m}$ ) is in mm, making it easy for collagen insertion. Processed somatic cells taken from milk were mixed with collagen gel at a ratio of 1:9 and transferred (1.5  $\mu\text{L}$ ) in pyramid-shaped wells (1.4 cm, 3.6 cm, 1 mm well), lower surface ( $200 \times 200 \mu\text{m}$ ), upper surface ( $1550 \times 1550 \mu\text{m}$ )) followed by incubation at 37  $^{\circ}\text{C}$  for 15 min (Figure 2A). Figure 2B shows a photograph of a well without and with somatic cells.

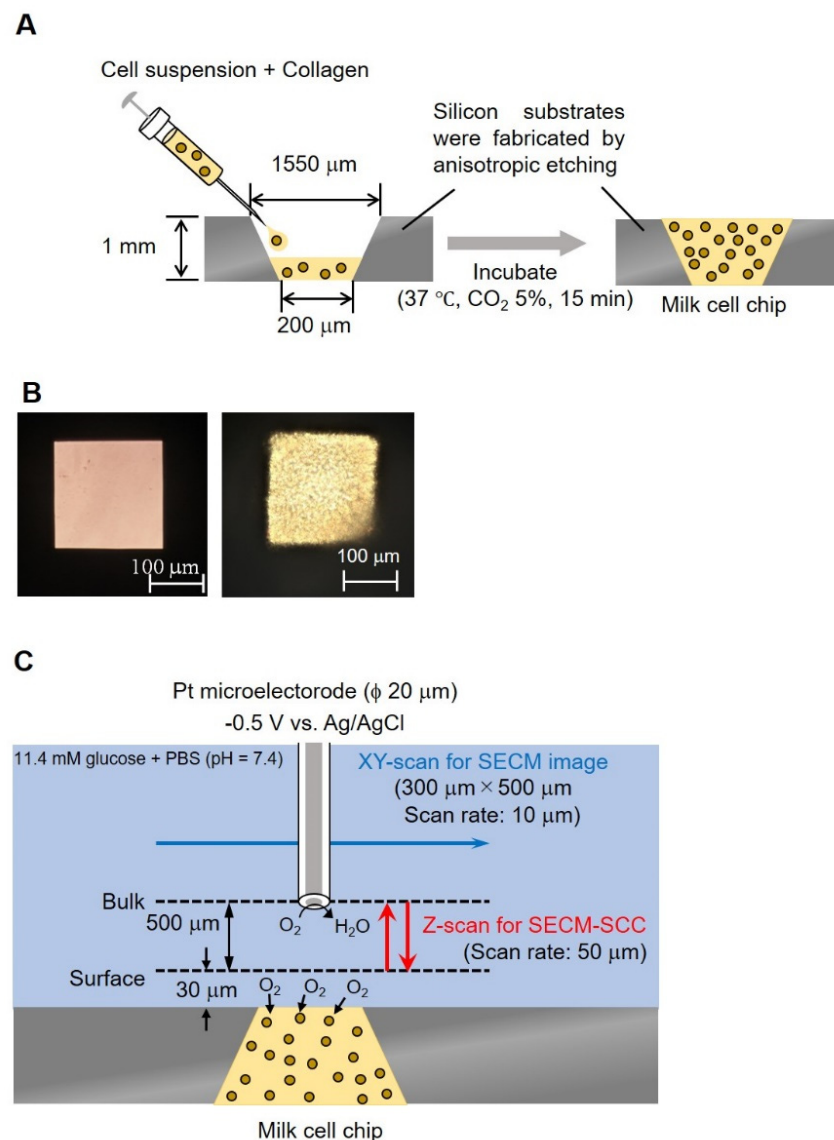


**Figure 2.** Conceptual diagram and photographs of milk cell chips. Schematic diagram of milk cell chips (A). Milk (–) and milk (+) (B). The experimental method of XY-scan and Z-scan (C). In the XY-scan, the distance between the microelectrode and the milk cell chip was set to 30  $\mu\text{m}$  or 160  $\mu\text{m}$  and scanned the range of 300  $\mu\text{m}$   $\times$  500  $\mu\text{m}$  while applying  $-0.5\text{ V vs. Ag/AgCl}$ . In the Z-scan,  $-0.5\text{ V vs. Ag/AgCl}$  was applied to the Pt microelectrode. The working electrode was held 30  $\mu\text{m}$  above the top of the well and scanned 500  $\mu\text{m}$  in the Z direction to measure respiration activity. The scan rate was kept at 50  $\mu\text{m/s}$ ; the number of scans was 3 and the sampling time was 100 ms.

#### 2.4. Understanding the Shape of the Oxygen Diffusion Layer

In order to understand the three-dimensional distribution of the oxygen concentration on the milk cell chip, the oxygen reduction currents in the XY-direction and the Z-direction were visualized while being held at the oxygen reduction potential. We used Pt microelectrodes ( $\phi\ 20\ \mu\text{m}$ ) as the working electrode, Ag/AgCl as the counter electrode and reference electrode, and 15 mL of 11.4 mM glucose-containing PBS as the measurement solution. By keeping the distance between the upper surface of the well and the microelectrodes at 30 or 160  $\mu\text{m}$  and scanning the vicinity of the upper surface of the well for 300  $\times$  500  $\mu\text{m}$  in the XY-direction, an image of the oxygen concentration distribution near the upper surface of the well was taken (Figure 2C). The scanning speed was 50  $\mu\text{m/s}$ , and the resolution was 10  $\mu\text{m}$ . The number of cells was kept at approximately  $3.00 \times 10^6$  cells/mL. To examine the minimum scanning range required for Z-scan, the accurate oxygen concentration



distribution in the vertical direction was measured by scanning in the vertical direction. The microelectrode was fixed at a position 20  $\mu\text{m}$  above the chip detection port. After the oxygen reduction current value stabilized, a 10  $\mu\text{m}$  upward scan was done at a rate of 10  $\mu\text{m}/\text{s}$ . This operation was repeated until the distance between the microelectrode and the chip reached 140  $\mu\text{m}$ .

### 2.5. SECM-SCC with Milk Cell Chip

Based on the results of the analysis of the Z-scan's scanning distance, the surface was determined to be 30  $\mu\text{m}$  above the milk cell chip. In the mastitis test method, it is important to discriminate between  $2 \times 10^5$  cells/mL, which is the criterion for mastitis, and lower. We used Pt microelectrodes ( $\phi$  20  $\mu\text{m}$ ) as the working electrode, Ag/AgCl as the counter electrode and reference electrode, and 15 mL of 11.4 mM glucose-containing PBS as the measurement solution. We applied  $-0.5$  V vs. Ag/AgCl to the Pt microelectrode. The microelectrode was held 30  $\mu\text{m}$  above the top of the well and 500  $\mu\text{m}$  in the Z-direction was scanned to measure respiratory activity. The sweep speed was kept at 50  $\mu\text{m}/\text{s}$ , the number of scans was 3, and the sampling time was 100 ms (Figure 2C). The microelectrode reciprocated between a position (surface) about 30  $\mu\text{m}$  above the surface of the milk cell chip and about 530  $\mu\text{m}$  (bulk) at intervals of 20 s. This experiment was performed on three samples, with cell numbers of  $1.10 \times 10^6$ ,  $5.50 \times 10^5$ , and  $5.50 \times 10^4$  cells/mL. These samples were prepared by diluting  $1.10 \times 10^6$  cells/mL from the same cow with the measurement solution.

In order to reach a simplified methodology, we also evaluated if centrifugation can be replaced by an alternative method. By inserting nanofibers into a syringe and passing raw milk without centrifugation, results were obtained by performing SECM-SCC. This has the added advantage of overall shortening of the sample preparation time.

### 2.6. Evaluation of Respiratory Burst Using SECM-SCC

Raw milk containing  $4.15 \times 10^6$  cells/mL somatic cells determined using flow cytometry at Miyagi Prefectural Livestock Association was evaluated in the absence and presence of 20 nM phorbol 12-myristate 13-acetate (PMA). PMA was used to induce respiratory burst, and comparative measurements were done. Other measurement conditions for the electrochemical system of SECM-SCC are the same as described in Section 2.5.

## 3. Results and Discussion

### 3.1. Correlation between Somatic Cell Count and Respiration Activity Using Inverted Cone-Shaped Well

The solid red line in Figure 3 shows the measurement result of  $6.00 \times 10^6$  cells/mL, and the blue dotted line shows the result of  $6.00 \times 10^5$  cells/mL, measured using the setup shown in Figure 1B. On the surface, the reduction current value was reduced by several tens of pA compared to the bulk, indicating that the dissolved oxygen concentration in the vicinity was reduced by the respiration of somatic cells. The current value at 0 s was about 20% higher than that at 200 and 400 s. This is because the scanning was started immediately after the voltage was applied to the working electrode, and the measurement was performed before the current value became stable. In this study, the value at 0 s was not used when calculating the current value difference ( $\Delta I$ ) between the bulk and the surface. As presented in Figure 3, the difference in oxygen reduction current value between the bulk and surface on the first cycle (round trip)  $|\Delta I_1|$  was 100 s when the distance between the microelectrode and the cell suspension was the largest and 200 s when it was the smallest. Similarly, the difference in oxygen reduction current value between the two points of the other two cycles (two round trips) were read, and the average  $|\Delta I|$  was calculated. The difference in oxygen reduction current values was found to be about 105 pA at  $6.00 \times 10^6$  cells/mL and about 20 pA at  $6.00 \times 10^5$  cells/mL. The amount of dissolved oxygen in the measured solution at room temperature was about 248  $\mu\text{M}$ , as measured in our laboratory. The oxygen reduction current value at this time was  $-1.76$  nA. The difference in oxygen concentration ( $\Delta C$ ) was calculated from  $|\Delta I|$  and is summarized in Table 1.

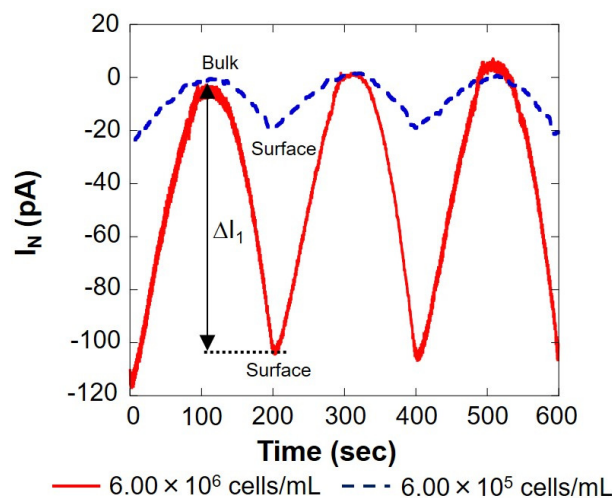


**Figure 3.** Changes in respiration activity with somatic cells.  $I_N$ : relative value of oxygen reduction current in bulk, which was set at 0 nA.

**Table 1.** Evaluation of somatic cells with inverted cone-shaped wells. The oxygen reduction current value difference between bulk and surface ( $\Delta I$ ) from Figure 3. The difference in oxygen reduction current was calculated using values at bulk ( $-1.76$  nA) and oxygen concentration ( $248$   $\mu$ M).

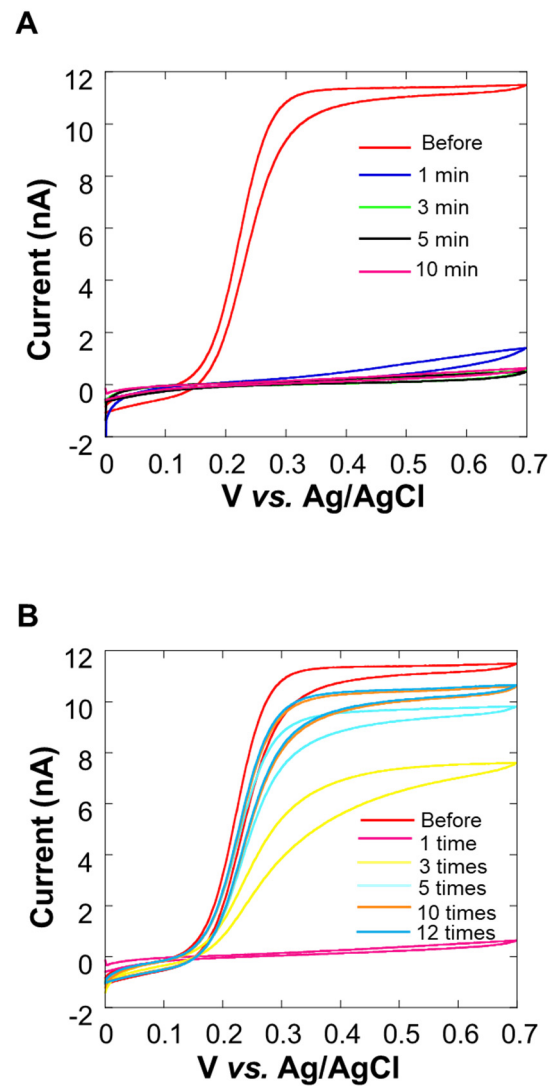
Cell Number (cells/mL)	$ \Delta I $ (pA)	$\Delta C$ ( $\mu$ M)
$6.00 \times 10^6$	105	15
$6.00 \times 10^5$	20	2.9

Table 1 shows that there is a correlation between the number of somatic cells and the difference in oxygen concentration. From this result, it was possible to evaluate the number of somatic cells in milk by measuring respiratory activity. However, at the same time, it was difficult to measure respiratory activity with a cell count fewer than  $10^5$  cells/mL.

### 3.2. Decrease in the Current Value over Time or Due to Collagen

In the cyclic voltammogram in Figure 4A, it can be observed that the current value decreases over time. After 10 min, the average current value at 0.5–0.7 V vs. Ag/AgCl was about 10% or less than it was before the experiment. We considered that this decrease in current value was the cause of insufficient sensitivity. In Figure 4B, it can be seen that the current value increases each time a cleaning pulse is applied (Figure 1D), and the waveform is close to sigmoidal. When the cleaning pulse was applied five times, the average current value at 0.5–0.7 V vs. Ag/AgCl was about 90% of the value observed before the experiment. However, the recovery of the current value was not seen when the number of times exceeded 10, and the value did not return to the original value before the experiment at the 12th time. For this reason, the appropriate use of cleaning pulses is effective for electrode activity.

Based on the experimental results over time by CV, it is considered that the adsorption of milk components on the electrode surface was the reason, so a method for suppressing the diffusion of milk components is required. We decided to embed cells using collagen [36] (Figure 2A), which is a biomaterial that inhibits the diffusion of milk components, and investigate the effect of suppressing the diffusion of milk components. Figure 5 shows the cyclic voltammogram before and after 10 min of the experiment. The average current value at 0.5–0.7 V vs. Ag/AgCl is about 99% of the current value before the experiment, and there is almost no change in the current value. From this, it is considered that the collagen embedding treatment can prevent the current value from decreasing over time.



**Figure 4.** Cyclic voltammogram of 0.0~0.7 V vs. Ag/AgCl in potassium ferrocyanide solution at 0 min, 1 min, 3 min, 5 min, and 10 min after the measurement of the Pt microelectrode. Oxygen reduction current was measured at a sample-electrode distance of 20  $\mu\text{m}$ .

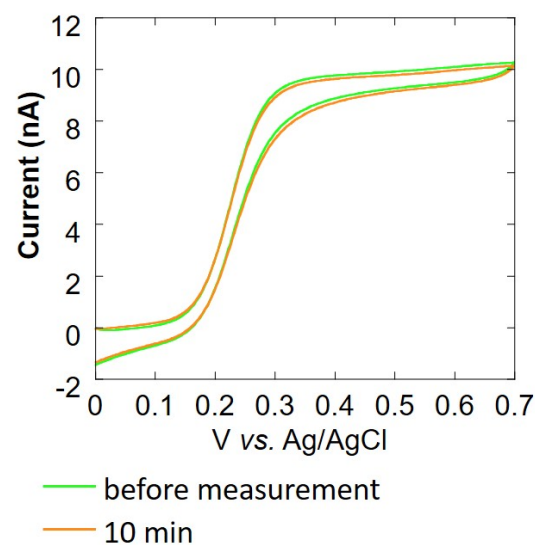


**Figure 5.** Evaluation of changes over time (in current value) by cyclic voltammetry upon collagen embedding.



### 3.3. Hemispherical Oxygen Diffusion Layer on Milk Cell Chip

The shape of the oxygen diffusion layer was estimated by taking two XY images on the milk cell chip and comparing them. In Figure 6A(a,b), the oxygen reduction current values are distributed almost in a circle. It is suggested that the cause of the distortion in the x-direction is that the oxygen diffusion layer on the chip is disturbed in the x-direction because the microelectrodes are scanned in the x-axis direction. The line segments ( $L_1$ ) and ( $L_2$ ) exist on the same x-coordinate. We set L as half the length at which the oxygen reduction currents of the line segments ( $L_1$ ) and ( $L_2$ ) are  $-1.4$  nA or less. We calculated  $r'$  using the three-square theorem, and both were about  $1.6 \times 10^2 \mu\text{m}$ . This result suggests that the oxygen concentration distribution exists as shown in Figure 7. These results show that a hemispherical oxygen diffusion layer is formed on the milk cell chip. Therefore, oxygen diffusion is considered to follow the spherical diffusion theory.

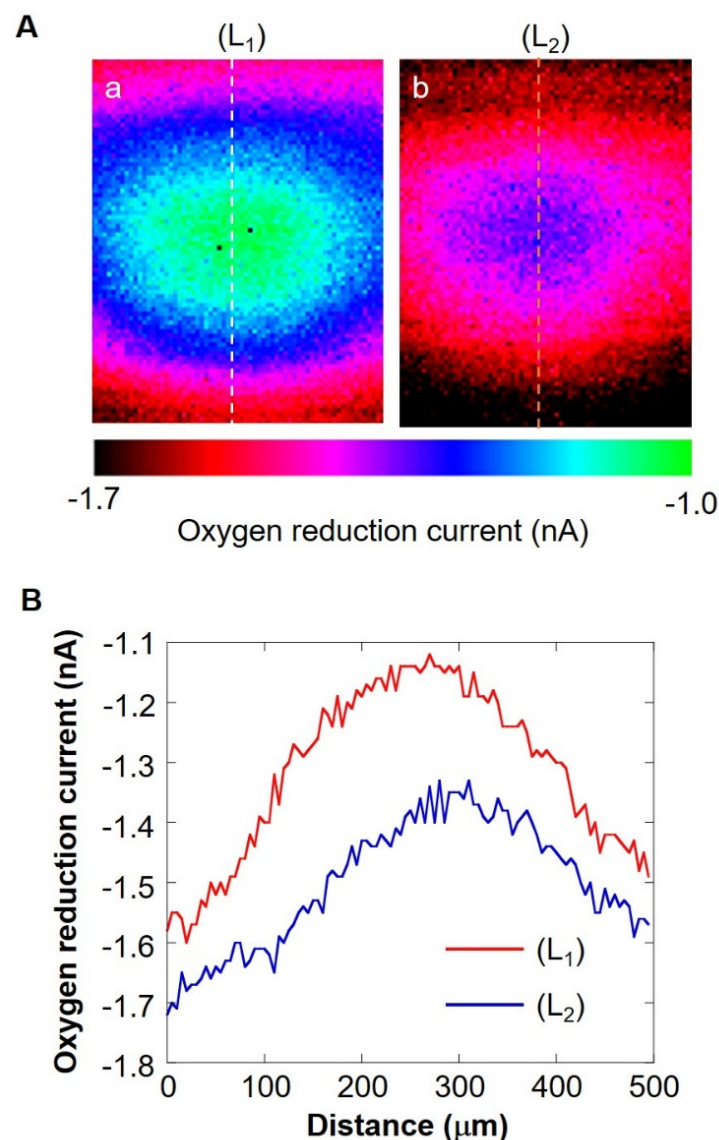


**Figure 6.** (A) XY-scan images showing the oxygen concentration distribution with the distance between Pt microelectrode and the cell chip of 30  $\mu\text{m}$  (a) and 160  $\mu\text{m}$  (b). Line ( $L_1$ ) and ( $L_2$ ) are on the same X coordinate. Graph (B) shows the oxygen reduction current values of line ( $L_1$ ) and line ( $L_2$ ).

Since the oxygen diffusion layer on the milk cell chip is hemispherical, we considered  $f$  as the oxygen diffusion flux ( $\text{mol}/\text{cm}^2$ ),  $D$  as the oxygen diffusion coefficient ( $2.18 \times 10^{-5} \text{cm}^2/\text{s}$ ), and  $C$  as the oxygen concentration of the surface ( $\text{mol}/\text{cm}^3$ ).  $C^*$  is the

bulk oxygen concentration ( $\text{mol}/\text{cm}^3$ ),  $r_s$  is the detection port radius (mm), and  $F$  is the oxygen consumption rate ( $\text{mol}/\text{s}$ ). We set  $R = r + r_s$ . The oxygen diffusion layer follows the hemispherical diffusion theory, and the initial conditions and boundary conditions are determined as follows:

$$t = 0, R \geq r_s \ (r \geq 0), C = C^*$$

$$t \geq 0, R \rightarrow \infty, C = C^*$$

$$t \leq 0, R = r_s \ (r = 0), C = C_s$$

Then, the overall respiration rate  $F$  is

$$F = 2\pi r_s D(C^* - C_s) \tag{1}$$

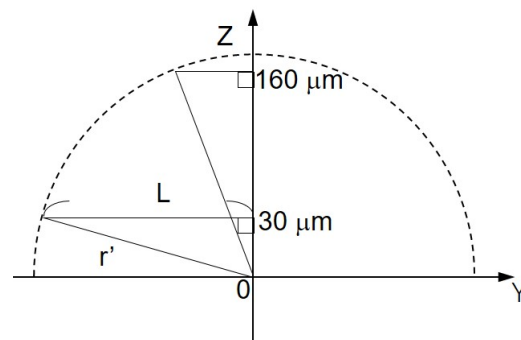


**Figure 7.** Schematic diagram of the oxygen concentration distribution on ZY plane.  $L$ , half the distance of the oxygen reduction current less than or equal to  $-1.4 \text{ nA}$ ;  $Z'$ , the distance between Pt microelectrode and the cell chip;  $r'$ , oblique side of the right triangle.

The numerical value at the bottom of the graph in Figure 8 shows the distance between the microelectrode and the chip (as shown in Figure 2C). After scanning, the current value was found to be increasing. In addition, the larger the distance between the microelectrode and the chip, the smaller the difference in value of current. This suggests that the oxygen consumption of the cells in the chip reduces the oxygen concentration near the detection port and forms a diffusion layer. Since there is almost no difference in current value when scanning from  $130 \mu\text{m}$  to  $140 \mu\text{m}$ , it is possible to compare the oxygen reduction current values at the point near the detection port and the point where the distance between the microelectrode and the chip is  $140 \mu\text{m}$  or more. It is considered that oxygen consumption of somatic cells in milk can be measured. In this study, the scanning range was set as  $30 \mu\text{m}$  to  $530 \mu\text{m}$ .

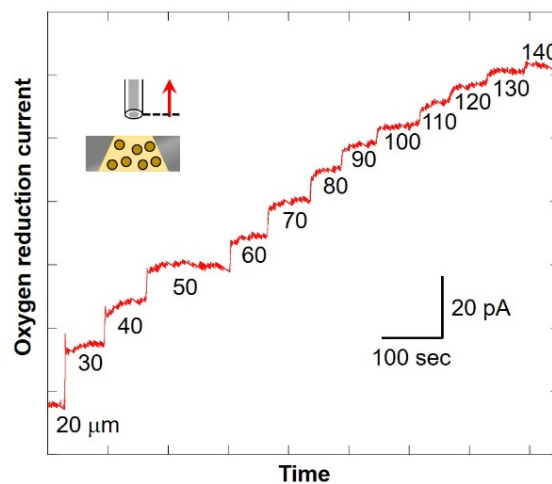


**Figure 8.** Changes in oxygen reduction current value in the Z-axis direction.

### 3.4. SECM-SCC and Calibration Curve Using Milk Cell Chip

We compared the respiratory activity of milk cell chips by cell number and examined the correlation with somatic cell number. Figure 9 shows SECM-SCC at three different cell concentrations. The red line, blue line, and green line show the measurement results for the difference in the number of cells of  $1.10 \times 10^6$  cells/mL,  $5.50 \times 10^5$  cells/mL, and  $5.50 \times 10^4$  cells/mL, respectively. When the microelectrode is located near the milk cell chip (surface) at 20 s intervals, an oxygen reduction current depending on the number of cells is obtained. In addition, it can be seen that it does not depend on the number of cells at the bulk position. This suggests that SECM-SCC using milk cell chips with collagen gel may measure in the range of  $10^4$  cells/mL to  $10^6$  cells/mL. Dissolved oxygen was set at  $25^\circ\text{C}$  ( $248\ \mu\text{M}$ ), the oxygen reduction current value ( $-1.7\ \text{nA}$ ) was set, and the respiration rate (F) was calculated by the concentration and Equation (1) in the same manner as in Section 3.1; the results are summarized in Table 2. The value of respiration rate calculated from the hemispherical diffusion equation reflects the respiratory activity of somatic cells. Therefore, it is suggested that the oxygen reduction current value depends on the number of somatic cells.

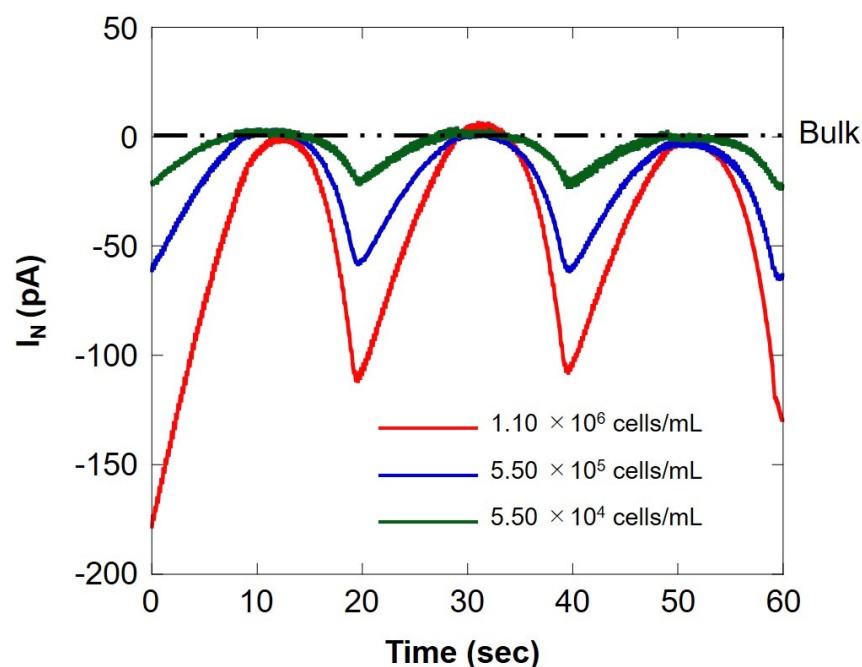


**Figure 9.** Comparison of the oxygen reduction currents measured via Z-scanning at three different cell concentrations. The red, blue, and green lines indicate the respiratory activity at a cell concentration of  $1.10 \times 10^6$  cells/mL,  $5.50 \times 10^5$  cells/mL, and  $5.50 \times 10^4$  cells/mL, respectively.  $I_N$ : relative value of oxygen reduction current in bulk, which was set at 0 nA.

**Table 2.** SECM-SCC with the milk cell chip. The respiration rate (F) is calculated using Equation (1).

Number of Cells (cells/mL)	$ \Delta I $ (pA)	$\Delta C$ ( $\mu\text{M}$ )	$F \times 10^{14}$ (mol/s/well)
$1.10 \times 10^6$	116	17	2.3
$5.50 \times 10^5$	70	10	1.4
$5.50 \times 10^4$	23	3.4	0.44

Figure 10 shows a preliminary calibration curve for measuring the number of somatic cells by evaluating respiratory activity. The oxygen reduction current value linearly depends on the number of cells between  $10^4$  cells/mL and  $10^6$  cells/mL. From this result, it is evident that the number of somatic cells can be measured by evaluating the respiratory activity using an electrochemical method. The results show that the difference in

respiration activity is due to the number of cells. SECM-SCC thus can be claimed to have sufficient sensitivity. In addition, it was possible to measure oxygen consumption in the same way as in Figure 9, with raw milk cell chips that were filtered using nanofibers instead of centrifugation to separate fat (Supplementary Figure S1).

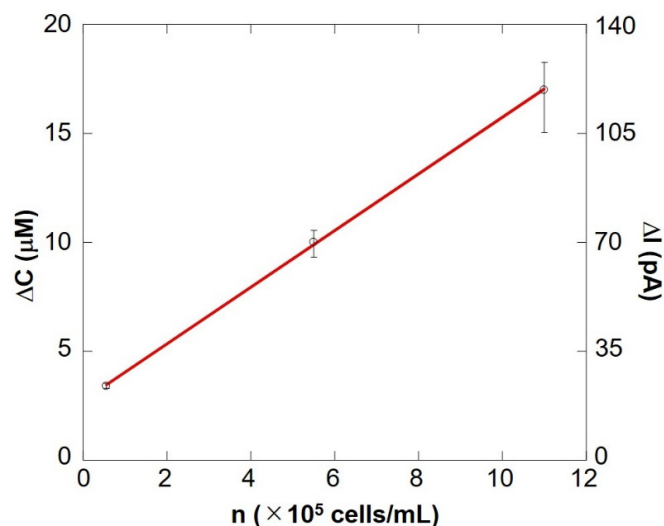


**Figure 10.** SECM-SCC calibration curve showing cell concentration vs. the change in oxygen concentration. The bar shows the standard deviation of each  $\Delta I$  value obtained from multiple scans of SECM-SCC ( $n = 3$ ).

### 3.5. Immune Cell Evaluation under Respiratory Burst Using SECM-SCC

Figure 11 shows a comparison of oxygen consumption of somatic cells in the milk cell chip using SECM-SCC during normal respiration and respiratory burst. It can be seen that the current value under PMA is increased about five times. This is because of the fact that PMA induces respiratory burst in immune cells such as monocytes and neutrophils. From these results, it is evident that the respiratory burst evaluation method using PMA in combination with SECM-SCC to specifically evaluate the immune cells in raw milk can be used for detection of latent breast inflammation and early stages of mastitis.

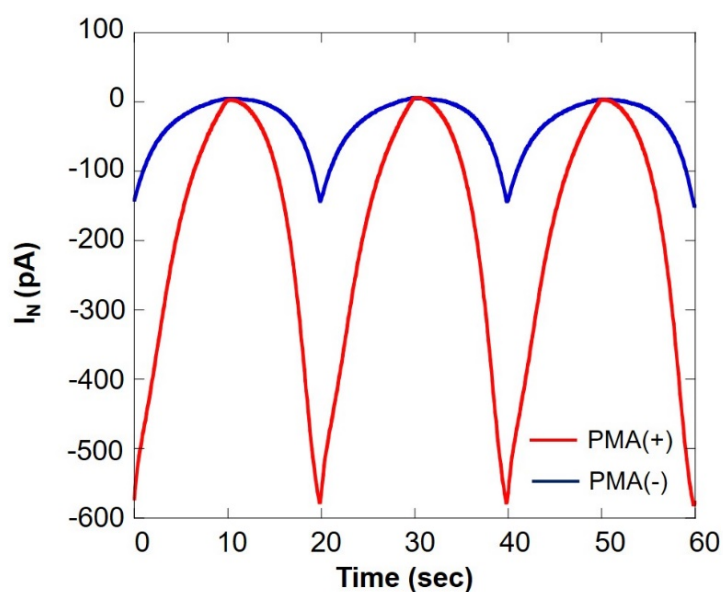


**Figure 11.** Comparison of oxygen consumption of somatic cells in milk cell chip using SECM-SCC during ordinary respiration (blue line) and during respiratory burst (red line)  $I_N$ : relative value of oxygen reduction current in bulk, which was set at 0 nA.

### 3.6. Bovine Examination by SECM-SCC

Figure 12 shows the results of an SECM-SCC study of milk samples. In the graph presented in Figure 12, the red and blue lines show the data from bovines diagnosed with different stage of mastitis. Because of scanning the microelectrode with SECM-SCC, notable differences were obtained at 20 s, 40 s, and 60 s. Table 3 shows the results of estimation of the number of somatic cells in the sample from the calibration curve in Figure 10.

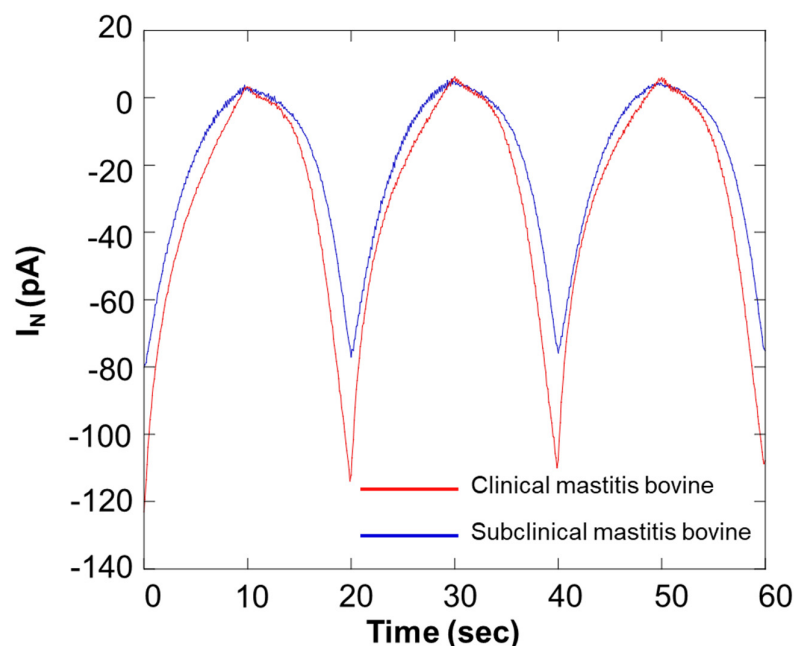


**Figure 12.** Comparison of respiration activity between bovines diagnosed with different stages of mastitis.  $I_N$ : relative value of oxygen reduction current in bulk, which was set at 0 nA.

**Table 3.** Comparison of bovines by SECM-SCC. The number of somatic cells was estimated from Figure 10.

	$ \Delta I $ (pA)	Number of Somatic Cells Estimated Using SECM-SCC (cells/mL)
Bovine sample 1	115	$1.08 \times 10^6$
Bovine sample 2	74	$6.20 \times 10^5$

## 4. Conclusions

Our results clearly show that the number of somatic cells can be measured by the evaluation of the respiratory activity. Because the degree of oxygen depletion is directly proportional to the number of cells, we can derive the number of cells in the milk. The chip device designed specifically for the dairy industry to be used at the farm was developed with the aim that it could serve as an effective method to access the quality of milk and/or to detect early onset of mastitis in buffalos, ensuring accuracy and cost effectiveness. The current assay suffers limitations due to the fact that it detects only live cells, and this can eventually lead to misuse of the technique and/or misinterpretation of results. Thus, the technique needs further development to pave the way to wider application.

**Supplementary Materials:** The following supporting information can be downloaded at: <https://www.mdpi.com/article/10.3390/biology11040549/s1>, Figure S1: The oxygen reduction current from somatic cells in the milk cell chip filtered using nanofibers and without centrifugation. The raw milk determined using flow cytometry at Livestock improvement association of Japan. Approximately 0.27 g of nanofibers was inserted into a 10 mL disposable syringe and 5 mL milk ( $6.5 \times 10^6$  cells/mL) was filtered through the syringe. SECM-SCC was performed in the same manner as in Section 2.5.



**Author Contributions:** Conceptualization, S.K.; methodology, S.K., R.K. and K.T.; validation, S.K. and A.P.; formal analysis, S.K. and A.P.; data curation, S.K., R.K. and K.T.; writing—original draft preparation, S.K., A.P. and R.K.; writing—review and editing, S.K. and A.P.; project administration, S.K. All authors have read and agreed to the published version of the manuscript.

**Funding:** AP is grateful for the funding from the European Regional Development Fund project “Plants as a tool for sustainable global development” (CZ.02.1.01/0.0/0.0/16\_019/0000827).

**Institutional Review Board Statement:** Not applicable.

**Informed Consent Statement:** Not applicable.

**Data Availability Statement:** Not applicable.

**Acknowledgments:** The authors would like to thank Masashi Kumagai, the director of Morinokuma Animal Clinic, Natori, Japan, and Sato Yoshiteru from Kakuda, Japan, for providing necessary assistance for the study.

**Conflicts of Interest:** The authors declare no conflict of interest.

## References

- Bradley, A. Bovine Mastitis: An Evolving Disease. *Vet. J.* **2002**, *164*, 116–128. [[CrossRef](#)] [[PubMed](#)]
- Abebe, R.; Hatiya, H.; Abera, M.; Megersa, B.; Asmare, K. Bovine mastitis: Prevalence, risk factors and isolation of *Staphylococcus aureus* in dairy herds at Hawassa milk shed, South Ethiopia. *BMC Vet. Res.* **2016**, *12*, 270. [[CrossRef](#)] [[PubMed](#)]
- Zigo, F.; Vasil, M.; Ondrašovičová, S.; Výrostková, J.; Bujok, J.; Pecka-Kielb, E. Maintaining Optimal Mammary Gland Health and Prevention of Mastitis. *Front. Vet. Sci.* **2021**, *8*, 607311. [[CrossRef](#)] [[PubMed](#)]
- Sah, K.; Karki, P.; Shrestha, R.D.; Sigdel, A.; Adesogan, A.T.; Dahl, G.E. MILK Symposium review: Improving control of mastitis in dairy animals in Nepal. *J. Dairy Sci.* **2020**, *103*, 9740–9747. [[CrossRef](#)] [[PubMed](#)]
- Pyörälä, S. New Strategies to Prevent Mastitis. *Reprod. Domest. Anim.* **2002**, *37*, 211–216. [[CrossRef](#)] [[PubMed](#)]
- Cobirka, M.; Tancin, V.; Slama, P. Epidemiology and Classification of Mastitis. *Animals* **2020**, *10*, 2212. [[CrossRef](#)] [[PubMed](#)]
- Sharma, N.; Singh, N.K.; Bhadwal, M.S. Relationship of Somatic Cell Count and Mastitis: An Overview. *Asian-Australas. J. Anim. Sci.* **2011**, *24*, 429–438. [[CrossRef](#)]
- Hillerton, J.E. *Redefining Mastitis Based on Somatic Cell Count, Bulletin of the International Dairy Federation No 345/1999: Quality and Safety of Raw Milk and Its Impact on Milk and Milk Products*; International Dairy Federation: Brussels, Belgium, 1999; pp. 4–6.
- Viguié, C.; Arora, S.; Gilmartin, N.; Welbeck, K.; O’Kennedy, R. Mastitis detection: Current trends and future perspectives. *Trends Biotechnol.* **2009**, *27*, 486–493. [[CrossRef](#)]
- Dohoo, I.; Leslie, K. Evaluation of changes in somatic cell counts as indicators of new intramammary infections. *Prev. Vet. Med.* **1991**, *10*, 225–237. [[CrossRef](#)]
- Chaiyotwittayakun, A.; Aiumlamai, S.; Chanlun, A.; Srisupa, S. Alternative Method for Determination of Milk Somatic Cell Count in Dairy Cow. In Proceedings of the 15th Congress of the Federation of Asian Veterinary Associations, Fava-Oie Joint Symposium on Emerging Diseases, Bangkok, Thailand, 27–30 October 2008; pp. 17–18.
- Zajac, P.; Zubricka, S.; Capla, J.; Zelenakova, L. Fluorescence microscopy methods for the determination of somatic cell count in raw cow’s milk. *Veterinární Med.* **2016**, *61*, 612–622. [[CrossRef](#)]
- Kim, K.-S.; Noh, H.-W.; Lim, S.-D.; Choi, C.-H.; Kim, Y.-J. Development of Rapid Somatic Cell Counting Method by Using Dye Adding NIR Spectroscopy. *Korean J. Food Sci. Anim. Resour.* **2008**, *28*, 63–68. [[CrossRef](#)]
- Albenzio, M.; Caroprese, M. Differential leucocyte count for ewe milk with low and high somatic cell count. *J. Dairy Res.* **2010**, *78*, 43–48. [[CrossRef](#)]
- Zigo, F.; Elečko, J.; Farkašová, Z.; Zigo, M.; Vasil, M.; Ondrašovičová, S.; Lenka, K. Preventive methods in reduction of mastitis pathogens in dairy cows. *J. Microbiol. Biotechnol. Food Sci.* **2019**, *9*, 121–126. [[CrossRef](#)]
- Barnum, D.A.; Newbould, F.H. The Use of the California Mastitis Test for the Detection of Bovine Mastitis. *Can. Vet. J. Rev. Vet. Can.* **1961**, *2*, 83–90.
- Ruegg, P.L. A 100-Year Review: Mastitis detection, management, and prevention. *J. Dairy Sci.* **2017**, *100*, 10381–10397. [[CrossRef](#)] [[PubMed](#)]
- Norberg, E. Electrical conductivity of milk as a phenotypic and genetic indicator of bovine mastitis: A review. *Livest. Prod. Sci.* **2005**, *96*, 129–139. [[CrossRef](#)]
- Sheldrake, R.; McGregor, G.; Hoare, R. Somatic Cell Count, Electrical Conductivity, and Serum Albumin Concentration for Detecting Bovine Mastitis. *J. Dairy Sci.* **1983**, *66*, 548–555. [[CrossRef](#)]
- Akhtar, M.; Guo, S.; Guo, Y.-F.; Zahoor, A.; Shaukat, A.; Chen, Y.; Umar, T.; Deng, G.; Guo, M. Upregulated-gene expression of pro-inflammatory cytokines (TNF-alpha, IL-1 beta and IL-6) via TLRs following NF-kappa B and MAPKs in bovine mastitis. *Acta Trop.* **2020**, *207*, 105458. [[CrossRef](#)]
- Halasa, T.; Nielen, M.; De Roos, A.P.W.; Van Hoorne, R.; de Jong, G.; Lam, T.J.G.M.; van Werven, T.; Hogeveen, H. Production loss due to new subclinical mastitis in Dutch dairy cows estimated with a test-day model. *J. Dairy Sci.* **2009**, *92*, 1315. [[CrossRef](#)]

22. Schukken, Y.H.; Wilson, D.J.; Welcome, F.; Garrison-Tikofsky, L.; Gonzalez, R.N. Monitoring udder health and milk quality using somatic cell counts. *Vet. Res.* **2003**, *34*, 579–596. [[CrossRef](#)]
23. Oviedo-Boyso, J.; Valdez-Alarcón, J.J.; Cajero-Juárez, M.; Ochoa-Zarzosa, A.; López-Meza, J.E.; Bravo-Patiño, A.; Baizabal-Aguirre, V.M. Innate immune response of bovine mammary gland to pathogenic bacteria responsible for mastitis. *J. Infect.* **2007**, *54*, 399–409. [[CrossRef](#)] [[PubMed](#)]
24. Alluwaimi, A.M.; Leutenegger, C.M.; Farver, T.B.; Rossitto, P.V.; Smith, W.L.; Cullor, J.S. The Cytokine Markers in Staphylococcus aureus Mastitis of Bovine Mammary Gland. *J. Vet. Med. Ser. B* **2003**, *50*, 105–111. [[CrossRef](#)] [[PubMed](#)]
25. Mehrzad, J.; Duchateau, L.; Burvenich, C. Phagocytic and bactericidal activity of blood and milk-resident neutrophils against Staphylococcus aureus in primiparous and multiparous cows during early lactation. *Vet. Microbiol.* **2009**, *134*, 106–112. [[CrossRef](#)] [[PubMed](#)]
26. Kimura, S.; Fukuda, J.; Tajima, A.; Suzuki, H. On-chip diagnosis of subclinical mastitis in cows by electrochemical measurement of neutrophil activity in milk. *Lab Chip* **2012**, *12*, 1309–1315. [[CrossRef](#)] [[PubMed](#)]
27. Bard, A.J.; Fan, F.R.F.; Kwak, J.; Lev, O. Scanning electrochemical microscopy. Introduction and principles. *Anal. Chem.* **1989**, *61*, 132–138. [[CrossRef](#)]
28. Bard, A.J.; Denuault, G.; Lee, C.; Mandler, D.; Wipf, D.O. Scanning electrochemical microscopy—A new technique for the characterization and modification of surfaces. *Acc. Chem. Res.* **1990**, *23*, 357–363. [[CrossRef](#)]
29. Shiku, H.; Shiraishi, T.; Aoyagi, S.; Utsumi, Y.; Matsudaira, M.; Abe, H.; Hoshi, H.; Kasai, S.; Ohya, H.; Matsue, T. Respiration activity of single bovine embryos entrapped in a cone-shaped microwell monitored by scanning electrochemical microscopy. *Anal. Chim. Acta* **2004**, *522*, 51–58. [[CrossRef](#)]
30. Shiku, H.; Torisawa, Y.-S.; Takagi, A.; Aoyagi, S.; Abe, H.; Hoshi, H.; Yasukawa, T.; Matsue, T. Metabolic and enzymatic activities of individual cells, spheroids and embryos as a function of the sample size. *Sens. Actuators B Chem.* **2005**, *108*, 597–602. [[CrossRef](#)]
31. Kai, T.; Zoski, C.G.; Bard, A.J. Scanning electrochemical microscopy at the nanometer level. *Chem. Commun.* **2018**, *54*, 1934–1947. [[CrossRef](#)]
32. Kaya, T.; Numai, D.; Nagamine, K.; Aoyagi, S.; Shiku, H.; Matsue, T. Respiration activity of Escherichia coli entrapped in a cone-shaped microwell and cylindrical micropore monitored by scanning electrochemical microscopy (SECM). *Analyst* **2004**, *129*, 529–534. [[CrossRef](#)]
33. Kikuchi, H.; Prasad, A.; Matsuoka, R.; Aoyagi, S.; Matsue, T.; Kasai, S. Scanning Electrochemical Microscopy Imaging during Respiratory Burst in Human Cell. *Front. Physiol.* **2016**, *7*, 25. [[CrossRef](#)] [[PubMed](#)]
34. Prasad, A.; Kikuchi, H.; Inoue, K.Y.; Suzuki, M.; Sugiura, Y.; Sugai, T.; Tomonori, A.; Tada, M.; Kobayashi, M.; Matsue, T.; et al. Simultaneous Real-Time Monitoring of Oxygen Consumption and Hydrogen Peroxide Production in Cells Using Our Newly Developed Chip-Type Biosensor Device. *Front. Physiol.* **2016**, *7*, 10. [[CrossRef](#)] [[PubMed](#)]
35. Kasai, S.; Shiku, H.; Torisawa, Y.-S.; Noda, H.; Yoshitake, J.; Shiraishi, T.; Yasukawa, T.; Watanabe, T.; Matsue, T.; Yoshimura, T. Real-time monitoring of reactive oxygen species production during differentiation of human monocytic cell lines (THP-1). *Anal. Chim. Acta* **2005**, *549*, 14–19. [[CrossRef](#)]
36. Torisawa, Y.-S.; Ohara, N.; Nagamine, K.; Kasai, S.; Yasukawa, T.; Shiku, H.; Matsue, T. Electrochemical Monitoring of Cellular Signal Transduction with a Secreted Alkaline Phosphatase Reporter System. *Anal. Chem.* **2006**, *78*, 7625–7631. [[CrossRef](#)] [[PubMed](#)]